Advances in Computer, Signals and Systems (2024)
Clausius Scientific Press, Canada

DOI: 10.23977/acss.2024.080606
ISSN 2371-8838 Vol. 8 Num. 6

A hybrid enhancement algorithm for polarised images based on a dark primary color prior

Qingze Zeng[1,a,*], Haotian Cao[1,b], Yunhe Xu[1,c]

[1]*School of Mechanical Engineering, Dalian Jiaotong University, Dalian, China*
[a]*18241905000@163.com*, [b]*2405765629@qq.com*, [c]*1299205059@qq.com*
[*]*Corresponding author*

Keywords: Underwater Polarization; Polarization Image

Abstract: As the further development of marine resources, the demand for underwater target detection has also increased. Conventional sonar detection cannot meet the high-precision visible light detection requirements. There are abundant impurity particles in natural water bodies, and traditional visible light detection techniques are seriously affected by scattering, resulting in short detection distances and low image quality. This paper utilizes the high anti-interference capability of polarized light and employs a polarized light detection imaging system to detect turbid underwater targets. To address the issues of large dark areas, low contrast, and color distortion in underwater images, a hybrid enhancement algorithm based on a dark primary color prior is proposed. The factors affecting polarized imaging in water are analyzed, and an image quality evaluation system is established. An improved median filter with average polarization is introduced, and the dark primary color prior algorithm is improved by introducing a compensation value δ and a quantitative parameter k. The experimental images are evaluated using EME and NIQE, and the results show that the EME value of the processed images is increased by about 4 times, and the NIQE value is decreased by nearly 35%.

1. Introduction

Traditional underwater imaging faces many problems such as low contrast between target and background light, color distortion, and overall decreased brightness may occur. Polarization imaging is a relatively new optical imaging technology. By utilizing the difference between the polarization of the target information light and the background scattered light, underwater polarization imaging technology can effectively weaken the influence of background scattered light on imaging.

In recent years, underwater polarization has developed rapidly, and algorithms for underwater image enhancement and restoration based on polarization detection technology have also received much attention. In 2005, Schechner derived the process of polarized light propagation underwater and established a passive underwater polarization imaging model. Based on Schechner's model, Huang et al. considered the polarization degree of the target light and expanded the application range of the model. Hu et al. proposed an underwater polarization imaging technology based on transmittance correction[1]. However, passive imaging may suffer from insufficient illumination.

Therefore, in 2009, Treibitz and Schechner established an active polarization imaging model, which is simpler and clearer in principle than the passive polarization imaging model[2]. In recent years, many researchers have been continuously optimizing the classic active polarization imaging model[3-5].

This paper utilizes the high anti-interference capability of polarized light and employs a polarized light detection imaging system to detect turbid underwater targets. To address the issues of large dark areas, low contrast, and color distortion in underwater images, a hybrid enhancement algorithm based on a dark primary color prior is proposed. An improved median filter with average polarization is introduced, and the dark primary color prior algorithm is improved by introducing a compensation value δ and a quantitative parameter K . The experimental images are evaluated using EME and NIQE, and the results show that the EME value of the processed images is increased by about 4 times, and the NIQE value is decreased by nearly 35%.

2. Experimental platform construction

To meet underwater use requirements, the article selected the TRIO50S-QC polarization camera from LUCID VISION LABS. The camera has a Sony IMX250MYR CMOS polarization sensor with 5MP resolution and 3.45μm pixel size. Each 4 pixels has 4 polarization filters at 0°, 90°, 45° and 135°, outputting pixel intensity and polarization angle. The camera can be powered via PoE (IEEE 802.3af) or 12-24 VDC external, with two options:

1) M8 GPIO 8-pin cable - one end with JST connector to camera, other end pre-stripped 3mm for soldering.

2) M12 to RJ45 IP67 Cat6a communication cable - connect to industrial PoE switch, which is then connected to a transformer.

The switch, also called a multi-port bridge, is a network device for optical-electrical signal forwarding. The article used a HIKVISION DS-3E0505SP-E 5-port full gigabit low-power PoE switch, suitable for the camera's short-distance indoor small-scale experiments due to its efficiency and stability.

To verify the effectiveness of the proposed method, this paper has built an active polarization imaging experimental platform. It is equipped with an LED lamp with a USP-50C0.4-38 linear polarizer, which serves as the active linear polarized light source

3. Hybrid Polarization Image Enhancement Algorithm

Median filtering effectively removes noise while overcoming the problem of blurring of image edge details that exists in low-pass filtering to a certain extent, the method uses the median of the grey values within the field of the centre pixel (including the centre pixel) instead of the centre pixel, however, there may be a problem of insufficient denoising, and the concept of the average deviation is introduced here. Assuming that the selection window is $k \times k$ (k is odd) and the centre pixel coordinates are $h(x,y)$, the average value within this window is:

$$A = \frac{1}{k \times k} \sum_{i=-\frac{k-1}{2}}^{\frac{k-1}{2}} \sum_{j=-\frac{k-1}{2}}^{\frac{k-1}{2}} h\left(x+i, y+j\right) \tag{1}$$

The average deviation is:

$$d=\frac{1}{k\times k}\left(\sum_{i=-\frac{k-1}{2}}^{\frac{k-1}{2}}\sum_{j=-\frac{k-1}{2}}^{\frac{k-1}{2}}|h(x+i,y+j)-A|\right) \tag{2}$$

Assuming that the grey value of the pixel point in the window is $f_t(x,y)\ (t=1,2,\dots,k^2)$, the average deviation can be used to limit the value of the pixel point; when $|f_t-A|\ll d$ the value of this pixel point is considered to be a valid value, it is retained unchanged; when $|f_t-A|>d$ the value of this pixel point is considered to be a noise, it is taken A to be the value of this point. Finally, the processed pixel values in the window are sorted to take the new median value.

First, a mathematical model is established for the hazy image:

$$I(x)=J(x)t(x)+A(1-t(x)) \tag{3}$$

Equation 3 represents the image degradation process caused by fog. Where $I(x)$ is the foggy image; $J(x)$ is the clear image after defogging; $t(x)$ is the medium transmittance; A is the global atmospheric light at infinity in the field of view. It is generally assumed that A by taking the invariant constant, both sides of Eq. 3 are divided A^C simultaneously:

$$\min_C\left(\min_{x\in\Theta}\left(\frac{I_C(x)}{A^C}\right)\right)=\ddot{t}(x)\min_C\left(\min_{x\in\Theta}\left(\frac{J_C(x)}{A^C}\right)\right)+\left(1-\ddot{t}(x)\right) \tag{4}$$

The dark primary color prior principle, there are always some pixel points with low intensity values, and that at least one of these pixel points has a low value within the color channel with a high probability of converging to 0. The dark primary color prior image model is built from this value, which can be expressed as:

$$J_{dark}(x)=\min_C\left(\min_{x\in\Theta}\left(J_C(x)\right)\right) \tag{5}$$

The predicted transmittance is:

$$\ddot{t}(x)=1-\min_C\left(\min_{x\in\Theta}\left(\frac{I_C(x)}{A^C}\right)\right) \tag{6}$$

The real scene, blue sky and white clouds in the sky also has a thin layer of fog, in order to make the image more realistic, here the introduction of the parameter $\omega(0\ll\omega\ll1)$, to increase the image hierarchy and depth of field effect, so:

$$\ddot{t}(x)=1-\omega\min_C\left(\min_{x\in\Theta}\left(\frac{I_C(x)}{A^C}\right)\right) \tag{7}$$

This paper is mostly an underwater polarization experiment, but the underwater model is very similar to the atmospheric model, so the dark primary color method can be applied to this paper. For easier understanding, the predicted transmittance model can be rewritten as:

$$\ddot{t}(x)=1-\omega\min_C\left(\min_{x\in\Theta}\left(\frac{I_C(x)}{B_{C,\infty}}\right)\right) \tag{8}$$

Where, $B_{C,\infty}$ denotes the background light at infinity, the selection rules are: 1) the brightest pixel point in the first 0.1% of the dark channel. 2) Due to the serious attenuation of underwater red light, the point with the largest red-green or red-blue intensity difference is selected among the pixel points satisfying 1).

When the predicted transmittance $\ddot{t}(x)$ is too low, the value $J(x)$ is too large, which will make the image excessive to the white field after defogging, set the threshold t_0, when $t < t_0$, make $t = t_0$; when $t \geq t_0$, keep t unchanged. At this time, the clarity formula is:

$$J(x) = \frac{I(x) - B_{C,\infty}}{\max(\ddot{t}(x), t_0)} + B_{C,\infty} \tag{9}$$

where t_0 is taken 0.1.

It is obtained by the derivation of the above equation:

$$\ddot{t}_{\text{actual}}(x) = \frac{1 - \omega \min_C \left(\min_{x \in \Theta} \left(\frac{I_C(x)}{B_{C,\infty}} \right) \right)}{1 - \min_C \left(\min_{x \in \Theta} \left(\frac{J_C(x)}{B_{C,\infty}} \right) \right)} \tag{10}$$

In some regions where the dark primary colour pixel value is not 0, so the predicted transmittance is smaller than the actual transmittance, which will lead to the clarified image being slightly darker than the real image as a whole, and a probability estimate δ is introduced here as an estimated refractive index

$$\ddot{t}(x) = 1 - \omega \min_C \left(\min_{x \in \Theta} \left(\frac{I_C(x)}{B_{C,\infty}} \right) \right) + \delta \tag{11}$$

In this paper, take $0.05 \leqslant \delta \leqslant 0.08$, when the image brightness is increased. If the compensated $t(x) > 1$, take $\ddot{t}(x) = 0.99$. Also in these areas, the image processed by the dark primary color method may appear color distortion. Based on this, the introduction of quantitative parameters K, if $|I - B_{C,\infty}| > K$, the region for the dark primary color area, the transmittance does not do processing; if $|I - B_{C,\infty}| < K$, the region for the bright area, the transmittance according K to do changes. At this time, the clarity formula is:

$$J(x) = \frac{I(x) - B_{C,\infty}}{\min\left(\max\left(\frac{K}{|I - B_{C,\infty}|}, 1\right) \cdot \max\left(\ddot{t}(x), t_0\right), 1\right)} + B_{C,\infty} \tag{12}$$

Two sets of images with darker field of view are processed using the algorithm of this paper and the results are shown in Figure 2. The evaluation metrics are shown in Table 1.

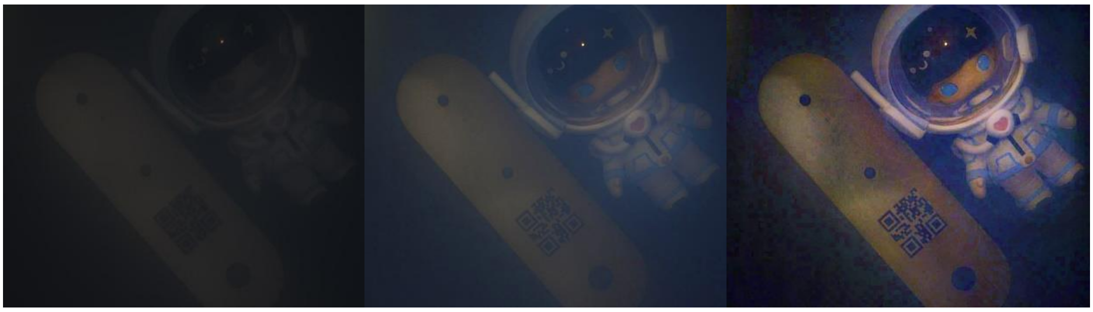

(a)Original image (b) Dark primary color (c) This paper

Figure 1: Comparison of algorithms in this paper.

Table 1: Evaluation of EME and information entropy

	EME			NIQE		
	(a)	(b)	(c)	(a)	(b)	(c)
First image	0.3886	0.9981	5.7670	9.2057	6.3060	4.0762
Second image	0.5864	0.9287	4.2034	12.5163	7.4356	4.8794

4. Conclusions

We have built an indoor underwater polarization imaging system and proposed a hybrid polarization image enhancement method. The experimental images are evaluated using EME and NIQE, and the results show that the EME value of the processed images is increased by about 4 times, and the NIQE value is decreased by nearly 35%.

References

[1] H. Hu, L. Zhao, B. Huang, X. Li, H. Wang, and T. Liu, "Enhancing Visibility of Polarimetric Underwater Image by Transmittance Correction," IEEE Photonics J, vol. 9, no. 3, Jun. 2017, doi: 10.1109/JPHOT.2017.2698000.

[2] T. Treibitz and Y. Y. Schechner, "Active polarization descattering," IEEE Trans Pattern Anal Mach Intell, vol. 31, no. 3, pp. 385–399, 2009, doi: 10.1109/TPAMI.2008.85.

[3] T. Yu, X. Wang, S. Xi, Q. Mu, and Z. Zhu, "Underwater polarization imaging for visibility enhancement of moving targets in turbid environments," Opt Express, vol. 31, no. 1, p. 459, Jan. 2023, doi: 10.1364/oe.477243.

[4] F. Liu et al., "Deeply seeing through highly turbid water by active polarization imaging," Opt Lett, vol. 43, no. 20, p. 4903, Oct. 2018, doi: 10.1364/ol.43.004903.

[5] Ronghua Li et al. Multi-Indicator reconstruction for underwater polarized image dehazing method, Optics and Lasers in Engineering, Volume 181,2024,108333,ISSN 0143-8166,https://doi.org/10.1016/j.optlaseng.2024.108333.